A Novel Objective Pathologic Criterion for Isolated Hypoganglionosis

玉城, 昭彦

This is a non-final version of an article published in final form in *American Journal of Surgical Pathology*.

Original Article

A novel objective pathological criterion for isolated hypoganglionosis

Akihiko Tamaki, MD[1,2], Kenichi Kohashi, MD, PhD[3], Koichiro Yoshimaru, MD, PhD[4], Yuko Hino, MD[1,2], Hiroshi Hamada, MD[1,2], Naonori Kawakubo, MD, PhD[2], Tomoaki Taguchi, MD, PhD[5], Tatsuro Tajiri, MD, PhD[2], Yoshinao Oda, MD, PhD[1]

[1]Department of Anatomic Pathology, Graduate School of Medical Sciences, Kyushu University, Fukuoka, Japan

[2]Department of Pediatric Surgery, Graduate School of Medical Sciences, Kyushu University, Fukuoka, Japan

[3]Department of Pathology, Graduate School of Medicine, Osaka Metropolitan University, Osaka, Japan

[4]Division of Pediatric Gastroenterology, Hepatology and Nutrition, Cincinnati Children's Hospital Medical Center, Cincinnati, Ohio, USA

[5]Fukuoka College of Health Sciences, Fukuoka, Japan

Corresponding author: Yoshinao Oda, MD, PhD, Department of Anatomic Pathology, Graduate School of Medical Sciences, Kyushu University, 3-1-1 Maidashi, Higashi-ku, Fukuoka-shi, Fukuoka, 812-8582, Japan

E-mail: oda.yoshinao.389@m.kyushu-u.ac.jp

Tel: +81-92-642-6061, FAX: +81-92-642-5968

CONFLICTS OF INTEREST

Guarantor of the article: Yoshinao Oda, MD, PhD.

Specific author contributions: A.T.: Conceptualization, Data curation, Formal analysis, Fund acquisition, Investigation, Project administration, Visualization, and Writing - original draft. K.K.: Conceptualization, Investigation, Project administration, Supervision, and Writing - Review and Editing. K.Y.: Conceptualization and Writing - Review. Y.H. and H.H.: Data curation and Investigation. N.K.: Formal analysis, Project administration, and Supervision. T.T.: Fund acquisition and Writing - Review. T.T.: Supervision and Writing - Review. Y.O.: Supervision and Writing - Review and Editing.

Conflicts of interest and Sources of funding: This study was supported by JSPS KAKENHI Grant Number 21K08597, AMED under Grant Number JP19ek0109361 and JP20ek0109361, and MHLW Program Grant Number JPMH 20FC1042. The authors report no conflict of interest.

ABSTRACT

Isolated hypoganglionosis (IHG) is histologically characterized by small numbers of myenteric ganglion cells and small myenteric ganglia; however, no numerical diagnostic criteria for IHG have been established. Therefore, this study aimed to develop quantitative pathological criteria for IHG. We evaluated 160 resected intestinal tissue specimens from 29 pediatric autopsy and 10 IHG cases. These specimens were obtained from the jejunum, ileum, ascending colon, transverse colon, and rectum. Morphological features of the myenteric ganglion cells and myenteric ganglia were quantified and analyzed in digitized HuC/HuD-immunostained and CD56-immunostained sections, respectively. Quantitative criteria were developed with a scoring system that used parameters with the area under the receiver operating characteristic curve (AUC) values >0.7 and sensitivity and specificity exceeding 70%. The selected parameters were the number of myenteric ganglion cells per cm and the number of myenteric ganglia with an area >2500 μm^2 per cm. The score for each parameter ranged from -1 to 2, and the total score of the scoring system ranged from -2 to 4. With a cutoff value of ≥2 (AUC, 0.98; 95% confidence interval [CI], 0.96–1.00), the scoring system had a sensitivity of 96% (95% CI, 0.82–1.00) and a specificity of 99% (95% CI, 0.95–1.00). We devised a novel pathological criterion based on the quantification of the number of myenteric ganglion cells and ganglia. Furthermore, this criterion showed high diagnostic accuracy and could lead to a definitive diagnosis of IHG in clinical practice.

KEYWORDS: isolated hypoganglionosis, criteria, HuC/HuD, CD56, scoring system

INTRODUCTION

Isolated hypoganglionosis (IHG) is a rare congenital disease that typically presents with persistent symptoms of severe intestinal obstruction in the neonatal period.[1-4] These symptoms are non-specific, and no imaging studies are useful for IHG diagnosis.[5] A definitive diagnosis requires a pathological examination, and IHG is histologically characterized by small numbers of myenteric ganglion cells, small-sized myenteric ganglia, and increased distance between myenteric ganglia (Figs. 1 and 2).[1,4,6-9] Due to these histological features, IHG has also been reported as " congenital myenteric hypoganglionosis."[1] Although IHG exhibits such quantitative histological findings, its quantitative pathological criteria have not yet been established.[2,9,10]

The lack of established quantitative criteria for IHG can be attributed to inadequate control data on myenteric plexus components, such as the number of myenteric ganglion cells per unit length or the area of each myenteric ganglion.[11] This lack of control data can be further attributed to the lack of standard methods for quantifying myenteric plexus components.[11,12] Although several studies have reported quantified data on myenteric plexus components, the results varied widely due to differences in the methods used for quantification.[1,7-9,13-22] Consequently, there are no reliable reproducible- and quantitative-morphological standards of myenteric plexus components, especially in children.[11,12] Therefore, regardless of the rarity of IHG, pathologists have had to determine quantitatively abnormalities in the myenteric plexus components based on their experience.

This study aimed to develop quantitative pathological diagnostic criteria for IHG that would be useful in clinical practice. To this end, using resected intestinal tissue from pediatric autopsy and IHG cases, we quantified and analyzed the morphological characteristics of myenteric ganglion cells and myenteric ganglia using methods that minimize subjectivity.

MATERIALS AND METHODS

Autopsy and isolated hypoganglionosis cases

This study included 29 pediatric autopsy cases aged <10 years examined at our institution and other collaborative institutions between January 2015 and December 2019 and 10 IHG cases clinicopathologically diagnosed between April 2005 and March 2022. Based on patient age, these cases were classified into three groups—Group 1, neonates (< 1-month-old); Group 2, infants (aged 1 month to under 1 year); and Group 3, toddlers or older (> 1 year).

Among autopsy cases, the patients who died of gastrointestinal-related disease or had episodes of bowel obstruction were excluded. In both groups, the resected intestinal tissue was fixed in 10% neutral buffered formalin and longitudinally cut into strips of at least 10 mm in length (autopsy group: 13–32mm, IHG group: 19–51mm). The examined sites were as follows: the jejunum (one-fifth of the proximal part of the small intestine), ileum (four-fifths of the proximal part of the small intestine), ascending colon (opposite side of the ileocecal valve), transverse colon (one-half of the large intestine), and rectum (the most distal part of the large intestine). In IHG cases, the surgical specimens from the above-mentioned sites taken in a single operation were used. The opt-out consent method was approved by the Institutional Review Board at Kyushu University (permission code: 2022-110).

Histological preparation

Specimens from both groups were embedded in paraffin wax. Formalin-fixed paraffin-embedded sections were cut into 4 μm-thick sections and used for hematoxylin and eosin staining and immunohistochemical staining using the streptavidin-biotin-peroxidase method. The primary antibodies used in this study were anti-HuC/HuD (mouse monoclonal, clone 16A11; A21271; dilution 1:400; Invitrogen, Waltham, MA, USA), which is useful for

accurate evaluation of myenteric ganglion cells,[1, 9-12] and anti-CD56 (mouse monoclonal, clone CD564; NCL-L-CD56-504; dilution 1:100; Leica Biosystems, Nussloch, Germany), which is useful for accurate evaluation of myenteric ganglia.[9]

Histopathological assessment and measurements

All stained sections were digitized using Leica Aperio GT 450 (Leica Biosystems, Tokyo, Japan). The digitized images were loaded onto the QuPath software (version 0.4.1),[23] and morphological measurements of the myenteric plexus components were performed using the software.

The quantified morphological features were the number of myenteric ganglion cells (/cm), area of myenteric ganglia (μm^2), distance between myenteric ganglia (μm), and diameter of the nucleus of myenteric ganglion cells (μm); these features were reported in previous studies.[1,7-9,13] Moreover, we counted the number of myenteric ganglia with an area >2500 μm^2 (/cm) using an eyepiece micrometer (U-OCMSQ10/10, Olympus, Tokyo, Japan) (Supplementary Fig. 1, Supplemental Digital Content 1). The cutoff value of 2500 μm^2 was determined based on the median area of the myenteric ganglia in autopsy cases. Morphological measurements of myenteric ganglion cells and myenteric ganglia were carried out with HuC/HuD-immunostained sections and CD56-immunostained sections, which are useful for histological evaluation.[1,9,24-26]

The measured myenteric ganglion cells were defined as cells (i) located between the inner circular and outer longitudinal layers of the muscularis externa, (ii) immunostained by HuC/HuD, and (iii) showing a nucleus with a visible contour of at least a semicircular shape (Fig. 3). The diameter of the nucleus of myenteric ganglion cells was measured only for cells with entirely visible nuclei (Fig. 3). The measured myenteric ganglia were defined as structures (i) placed between the inner circular and outer longitudinal layers of the muscularis

externa, (ii) immunostained by CD56, and (iii) consisting of one or more ganglion cells, glial cells, and nerve fibers (Fig. 3).

All morphological measurements were performed by a single pathologist (A.T.) who executed seven pilot measurements of the number of myenteric ganglion cells in three different sections and confirmed stable values before conducting this study. To achieve objectivity, when there was any doubt about the judgment, a consensus meeting was held between the two pathologists (A.T. and K.K.), and the data was adopted based on mutual agreement.

Statistical analysis

Patient demographic data and morphological analysis results are presented as median (range) and median (interquartile range), respectively. Data distributions were evaluated using histograms and box plots. In the analyses of the area of the myenteric ganglia and the distance between myenteric ganglia, log-transformed values were used to create and assess histograms and box plots. The differences and correlations between autopsy and IHG cases were assessed using the Brunner–Munzel Test and Spearman's rank correlation coefficient (r_s), respectively. Interpretation of the correlation coefficient (r_s) was as follows (in absolute numbers): <0.2, poor; 0.2–0.5, fair; 0.5–0.8, strong; and 0.8–1.0, very strong.[27] Receiver operating characteristic (ROC) curve analysis was used to assess the diagnostic accuracy. The area under the ROC curve (AUC) was interpreted as follows: 0.5–0.70, no to low diagnostic accuracy; 0.70–0.90, moderate diagnostic accuracy; and ≥0.90, high diagnostic accuracy.[28]

All tests were two-sided, and *P*-values ≤ 0.05 were considered statistically significant. All statistical analyses were performed using EZR version 1.55 (Saitama Medical Center, Jichi Medical University, Saitama, Japan).[29]

Scoring system development

A quantitative pathological diagnostic criterion was developed using a scoring system. The parameters of the scoring system were to satisfy the following conditions: (i) moderate or higher diagnostic accuracy (AUC ≥ 0.7) and (ii) sensitivity and specificity, both exceeding 70%. The parameters satisfying the above-mentioned conditions were the number of myenteric ganglion cells (/cm) and that of myenteric ganglia with an area >2500 μm^2 (/cm).

The scoring method for the number of ganglion cells (/cm) and the number of myenteric ganglia with an area >2500 μm^2 (/cm) is shown in Table 1; these scores were named N-score and S-score, respectively. The total score of the scoring system was the sum of the N- and S-scores and ranged from -2 to 4 (Table 1).

Using this scoring system, we scored all specimens and evaluated the diagnostic accuracy using ROC curve analysis, the AUC values, and their 95% confidence intervals (CIs). The optimal diagnostic cutoff value was determined using the Youden Index. Sensitivity, specificity, accuracy, positive predictive value (PPV), and negative predictive value (NPV) were also calculated.

RESULTS

The demographic data of the autopsy and IHG cases are summarized in Table 2. Autopsy cases included cases from groups 1 to 3, but there were no IHG cases with bowel resection in the neonatal period, hence IHG cases did not include cases from group 1 (neonatal cases). The proportion of patients in group 3 (toddlers or older cases) and the median age were higher in IHG cases than in autopsy cases; 160 specimens were evaluated, of which 132 and 28 were from autopsy and IHG cases, respectively.

Number of myenteric ganglion cells (cells/cm)

In autopsy cases, the number of myenteric ganglion cells tended to decrease with increasing age in months (r_s = -0.389, P < 0.001) and increasing age group (r_s = -0.363, P < 0.001; Fig. 4; Supplementary Table 1, Supplemental Digital Content 2). In evaluations based on the sampling site, this parameter increased from the jejunum to the rectum (r_s = 0.287, P < 0.001; Fig. 4; Supplementary Table 2, Supplemental Digital Content 3). The number of myenteric ganglion cells in the IHG group was significantly smaller than that in the autopsy group (P < 0.001; Table 3). At a cutoff value of ≤18.7, the ROC curve analysis yielded an AUC of 0.87 (95% CI, 0.81–0.93), with sensitivity and specificity of 71% and 86%, respectively (Fig. 5).

Area of myenteric ganglia (μm^2)

In autopsy cases, the area of the myenteric ganglia showed no correlation with age in months (r_s = 0.185, P < 0.001), age group (r_s = 0.174, P < 0.001; Fig. 4; Supplementary Table 1, Supplemental Digital Content 2), and sampling site (r_s = 0.186, P < 0.001; Fig. 4; Supplementary Table 2, Supplemental Digital Content 3). The area of the myenteric ganglia was significantly smaller in IHG cases than in autopsy cases (P < 0.001); the median area in IHG cases was one-third of that in the autopsies (Table 3). At a cutoff value of ≤1875 (log1875 = 3.27), the ROC curve analysis indicated an AUC of 0.75 (95% CI, 0.74–0.77), with sensitivity and specificity of 85% and 58%, respectively (Fig. 5).

Distance between myenteric ganglia (μm)

In autopsy cases, the distance between the myenteric ganglia showed no correlation with age in months (r_s = 0.118, P < 0.001), age group (r_s = 0.114, P < 0.001; Fig. 4; Supplementary Table 1, Supplemental Digital Content 2), and sampling site (r_s = -0.061, P <

0.001; Fig. 4; Supplementary Table 2, Supplemental Digital Content 3). Most measured distances between the myenteric ganglia were <1000 μm (log1000 = 3; Fig. 5).

The distance between the myenteric ganglia was significantly longer in IHG cases than in the autopsy group ($P < 0.001$); the median of IHG cases was almost twice that of the autopsies (Table 3). At a cutoff value of ≤435 (log435 = 2.64), the ROC curve analysis revealed an AUC of 0.65 (95% CI, 0.63–0.67), with sensitivity and specificity of 41% and 87%, respectively (Fig. 5).

Diameter of the nucleus of myenteric ganglion cells (μm)

In autopsy cases, the diameter of the nucleus of myenteric ganglion cells tended to increase with increasing age ($r_s = 0.236$, $P < 0.001$) and age groups ($r_s = 0.220$, $P < 0.001$; Fig. 4; Supplementary Table 1, Supplemental Digital Content 2). However, it showed no correlation with sampling sites (Fig. 4; Supplementary Table 2, Supplemental Digital Content 3).

The histogram showed almost the same distribution when comparing autopsy and IHG cases (Fig. 5). The diameter of the nucleus of myenteric ganglion cells was significantly larger in IHG cases than in autopsies ($P < 0.001$), but the difference in the median values of both groups was <1 μm (Table 3). At a cutoff value of ≤7.9, the ROC curve analysis yielded an AUC of 0.63 (95% CI, 0.60–0.65), with sensitivity and specificity of 75% and 45%, respectively (Fig. 5).

Number of myenteric ganglia with an area greater than 2500 μm^2 (ganglia/cm)

In autopsy cases, the number of myenteric ganglia with an area >2500 μm^2 showed no correlation with age in months ($r_s = 0.066$, $P = 0.446$) and the age group ($r_s = 0.055$, $P = 0.528$; Fig. 4; Supplementary Table 1, Supplemental Digital Content 2). However, this

parameter tended to increase from the jejunum to the rectum (r_s = 0.404, P < 0.001; Fig. 4; Supplementary Table 2, Supplemental Digital Content 3) and was significantly smaller in IHG cases than in autopsies (P < 0.001; Table 3). At a cutoff value of ≤3.6, the ROC curve analysis indicated an AUC of 0.99 (95% CI, 0.98–1.00), with sensitivity and specificity of 93% and 98%, respectively (Fig. 5).

Scoring system

We applied this scoring system to all 160 specimens; the results in IHG cases are shown in Table 4. At the optimal cutoff score of ≥2, the ROC analysis indicated an AUC of 0.98 (95% CI, 0.96–1.00; Supplementary Fig. 2, Supplemental Digital Content 4) and sensitivity and specificity of 96% (95% CI, 0.82–1.00) and 99% (95% CI, 0.95–1.00), respectively. The accuracy, PPV, and NPV were 98% (95% CI, 0.95–1.00), 93% (95% CI, 0.77–0.99), and 99% (95% CI, 0.96–1.00), respectively.

DISCUSSION

In this study, we developed a novel pathological diagnostic criterion for IHG by using a scoring system based on its histological features. This criterion offered two main advantages—a high degree of diagnostic accuracy and the ability to be scored using optical microscopes without any image analysis software. Thus, this criterion can be useful for diagnosing IHG in clinical practice. To the best of our knowledge, this is the first study to devise quantitative pathological criteria for IHG.

Previous reports could not be considered as reliable control data for children due to lack of objectivity, reproducibility, and clinical usefulness in the following aspects: the data were obtained from patients with a large age range, including adult cases[13-15,20,21]; evaluations were performed with HE staining alone[8,13] or with staining methods that are no longer in

use[7,14,16,19,22]; the use of whole-mount preparations[15,19]; and no definition of the myenteric plexus components to be counted.[7,8,15,17-29]

Therefore, to collect reliable data, we quantified myenteric plexus components by selecting pediatric autopsy cases as a control group, matching tissue-sampling sites between the two groups, evaluating neuron-specific-immunostained specimens, using longitudinally resected intestinal tissue, and defining the myenteric plexus components to be counted. Furthermore, we conducted measurement training to reduce measurement variability before starting this study. These methods have been reported to ensure the objectivity and reproducibility of measurements.[11,12] We concluded that our methods minimized subjectivity and that our data were valid.

The number of myenteric ganglion cells per cm may be used as a screening parameter for IHG diagnosis because of its moderate diagnostic accuracy and simplicity of measurement. Previous reports have described mean values of the number of myenteric ganglion cells evaluated using HuC/HuD-immunostained sections in IHG cases as 23.3 and 30.1 ganglion cells per cm.[1,9] Our cutoff value of ≤18.7/cm was smaller than the above-mentioned values and was considered reasonable as an abnormal decrease.

Moreover, despite the absence of neonates in IHG cases, this cutoff value may still be applicable to them. An analysis of autopsy cases revealed a negative correlation between the number of myenteric ganglion cells and age (in months). Notably, a similar trend has been reported previously.[19] Another study showed that the number of myenteric ganglion cells in IHG patients decreased from the neonatal period and did not increase with growth.[8] This indicates that the number of myenteric ganglion cells may peak during the neonatal period, and our cutoff value can be applied to neonates.

The area of the myenteric ganglia showed moderate diagnostic accuracy in ROC analysis but unsatisfactory sensitivity and specificity, which could be attributed to the wide

distribution of data in autopsy cases and the overlapped distribution in both groups. Although some studies have reported on the total area of the myenteric ganglia per unit length,[7,9] none mentioned the area of each individual ganglion, and there were no data to refer to. We observed that IHG cases had fewer myenteric ganglia with an area >the median in autopsy cases (2448 μm^2) and thus defined another parameter—the number of myenteric ganglia with an area >2500 μm^2/cm. This parameter can be measured using an optical microscope with an eyepiece micrometer showing high diagnostic accuracy.

The distance between the myenteric ganglia was significantly longer in IHG cases than in autopsy cases, which was consistent with the histological IHG features. A previous study reported similar results, albeit with different methods.[7] Conversely, the ROC analysis of this parameter showed low diagnostic accuracy, as data distribution widely overlapped in both groups. Previous studies have never reported the diagnostic accuracy of this parameter, and none could be used as reference data.

The diameter of the nucleus of myenteric ganglion cells was significantly larger in IHG cases than in autopsy cases. In autopsy cases, this parameter tended to increase with increasing age; a previous study has reported a similar trend in IHG cases.[8] This indicated that this result was influenced by the higher percentage of IHG cases >1 year in the autopsy group and the large sample size of this parameter. Moreover, the ROC analysis of this parameter showed low diagnostic accuracy because the data distribution overlapped widely in both groups. The difference in the median values in both groups was <1 μm, and this parameter was not clinically significant.

This study had several limitations. First, it included a small number of IHG cases, and external validation could not confirm the findings. However, IHG is a rare disease, and only three studies, including the present one, have collected information from more than 10 IHG cases.[1,9] Therefore, data from more IHG cases across multiple institutions are required for

313 further validation. Second, an observer bias may have occurred in this study. However, to
314 minimize subjectivity, we evaluated specimens using methods that have been recommended
315 to maintain objectivity and reproducibility,[11,12] and two pathologists (A.T. and K.K.) resolved
316 discrepancies in consensus. Digitized images were useful in discussing the judgment.
317 Finally, because only surgical specimens were included in this study, it was unclear whether
318 the criteria could be applied to biopsy specimens. Therefore, further validation using biopsy
319 specimens is warranted.

320 In conclusion, we devised a novel objective pathological criterion using a scoring
321 system based on myenteric ganglion cells and ganglia numbers. This criterion showed high
322 diagnostic accuracy and could be used for IHG definitive diagnosis in clinical practice.

323

324 **Acknowledgments**

325 *The authors thank Dr. Atsuko Nakazawa (Department of Clinical Research, Saitama*
326 *Children's Medical center, Saitama, Japan) and Dr. Iwao Nakazato (Department of*
327 *Pathology, Okinawa Prefectural Nanbu Medical Center and Children's Medical Center,*
328 *Okinawa, Japan) for providing the materials and the autopsy records. The authors also thank*
329 *all members of the Department of anatomic pathology, Graduate School of Medical Sciences,*
330 *Kyushu University. We would like to thank Editage (www.editage.com) for English language*
331 *editing.*

332

REFERENCES

1. Kapur RP, Bellizzi AM, Bond S, et al. Congenital myenteric hypoganglionosis. *Am J Surg Pathol.* 2021;45:1047–1060.
2. Friedmacher F, Puri P. Classification and diagnostic criteria of variants of Hirschsprung's disease. *Pediatr Surg Int.* 2013;29:855–872.
3. Dingemann J, Puri P. Isolated hypoganglionosis: Systematic review of a rare intestinal innervation defect. *Pediatr Surg Int.* 2010;26:1111–1115.
4. Kobayashi H, Yamataka A, Lane GJ, et al. Pathophysiology of Hypoganglionosis. *J Pediatr Gastroenterol Nutr.* 2002;34:231–235.
5. Watanabe Y, Kanamori Y, Uchida K, et al. Isolated hypoganglionosis: Results of a nationwide survey in Japan. *Pediatr Surg Int.* 2013;29:1127–1130.
6. Munakata K, Okabe I, Morita K. Histologic Studies of rectocolic aganglionosis and allied diseases. *J Pediatr Surg.* 1978;13:67–75.
7. Meier-Ruge W, Brunner L, Engert J, et al. A correlative morphometric and clinical investigation of hypoganglionosis of the colon in children. *Eur J Pediatr Surg*. 1999;9:67–74.
8. Taguchi T, Masumoto K, Ieiri S, et al. New classification of hypoganglionosis: congenital and acquired hypoganglionosis. *J Pediatr Surg.* 2006;41:2046–2051.
9. Yoshimaru K. Immunostaining for Hu C/D and CD56 is useful for a definitive histopathological diagnosis of congenital and acquired isolated hypoganglionosis. *Virchows Archiv.* 2017;470:679–685.
10. Muto M, Matsufuji H, Taguchi T, et al. Japanese clinical practice guidelines for allied disorders of Hirschsprung's disease, 2017. *Pediatr Int.* 2018;60:400–410.
11. Knowles CH, Veress B, Kapur RP, et al. Quantitation of cellular components of the enteric nervous system in the normal human gastrointestinal tract - report on behalf of

the Gastro 2009 International Working Group. *Neurogastroenterol Motil* 2011;23:115–124.

12. Knowles CH, de Giorgio R, Kapur RP, et al. Gastrointestinal neuromuscular pathology: Guidelines for histological techniques and reporting on behalf of the Gastro 2009 International Working Group. *Acta Neuropathol.* 2009;118:271–301.
13. Smith V V. Intestinal Neuronal Density in Childhood: A baseline for the objective assessment of hypo- and hyperganglionosis. *Pediatr Pathol.* 1993;13:225–237.
14. Yu CS, Kim HC, Hong HK, et al. Evaluation of myenteric ganglion cells and interstitial cells of Cajal in patients with chronic idiopathic constipation. *Int J Colorectal Dis.* 2002;17:253–258.
15. Wedel T, Roblick U, Gleifl J, et al. Organization of the enteric nervous system in the human colon demonstrated by wholemount immunohistochemistry with special reference to the submucous plexus. *Anat Anz.* 1999;181:327–337.
16. Meier-Ruge WA, Brunner LA. Morphometric assessment of Hirschsprung's disease: Associated hypoganglionosis of the colonic myenteric plexus. *Pediatr Dev Pathol.* 2001;4:53–61.
17. Scharli AF, Sossai R. Hypoganglionosis. *Semin Pediatr Surg.* 1998;7:187–191.
18. Csendes A, Smok G, Braghetto I, et al. Histological studies of Auerbach's plexuses of the oesophagus, stomach, jejunum, and colon in patients with achalasia of the oesophagus: Correlation with gastric acid secretion, presence of parietal cells and gastric emptying of solids. *Gut* 1992;33:150–154.
19. Wester T, O'Briain DS, Puri P. Notable postnatal alterations in the myenteric plexus of normal human bowel. *Gut* 1999;44:666–674.

20. Iwase H, Sadahiro S, Mukoyama S, et al. Morphology of myenteric plexuses in the human large intestine: comparison between large intestines with and without colonic diverticula. *J Clin Gasterol.* 2005;39:674–678.
21. T. Wedel, U. J. Roblick, H.-J. Krammer. Oligoneuronal hypoganglionosis in patients with idiopathic slow-transit constipation. *Dis Colon Rectum* 2002;45:54–62.
22. Krishnamurthy S, Heng Y, Shuffler MD. Chronic intestinal pseudo-obstruction in infants and children caused by diverse abnormalities of the myenteric plexus. *Gasteroenterology* 1993;104:1398–1408.
23. Bankhead P, Loughrey MB, Fernández JA, et al. QuPath: Open source software for digital pathology image analysis. *Sci Rep.* 2017;7:16878.
24. Ganns D, Schrodl F, Neuhuber W, et al. Investigation of general and cytoskeletal markers to estimate numbers and proportions of neurons in the human intestine. *Histol Histopathol*. 2006;21:41–51.
25. Swaminathan M, Kapur RP. Counting myenteric ganglion cells in histologic sections: An empirical approach. *Hum Pathol.* 2010;41:1097–1108.
26. Taguchi T, Ieiri S, Miyoshi K, et al. The incidence and outcome of allied disorders of Hirschsprung's disease in Japan: Results from a nationwide survey. *Asian J Surg.* 2017;40:29–34.
27. Gust L, D'journo XB. The use of correlation functions in thoracic surgery research. *J Thorac Dis.* 2015;7:E11–E15.
28. Grzybowski M, Younger JG. Statistical methodology: III. Receiver operating characteristic (ROC) curves. *Acad Emerg Med.* 1997;4:818–826.
29. Kanda Y. Investigation of the freely available easy-to-use software "EZR" for medical statistics. *Bone Marrow Transplant.* 2013;48:452–458.

406 **FIGURES**
407
408 **FIGURE 1.**

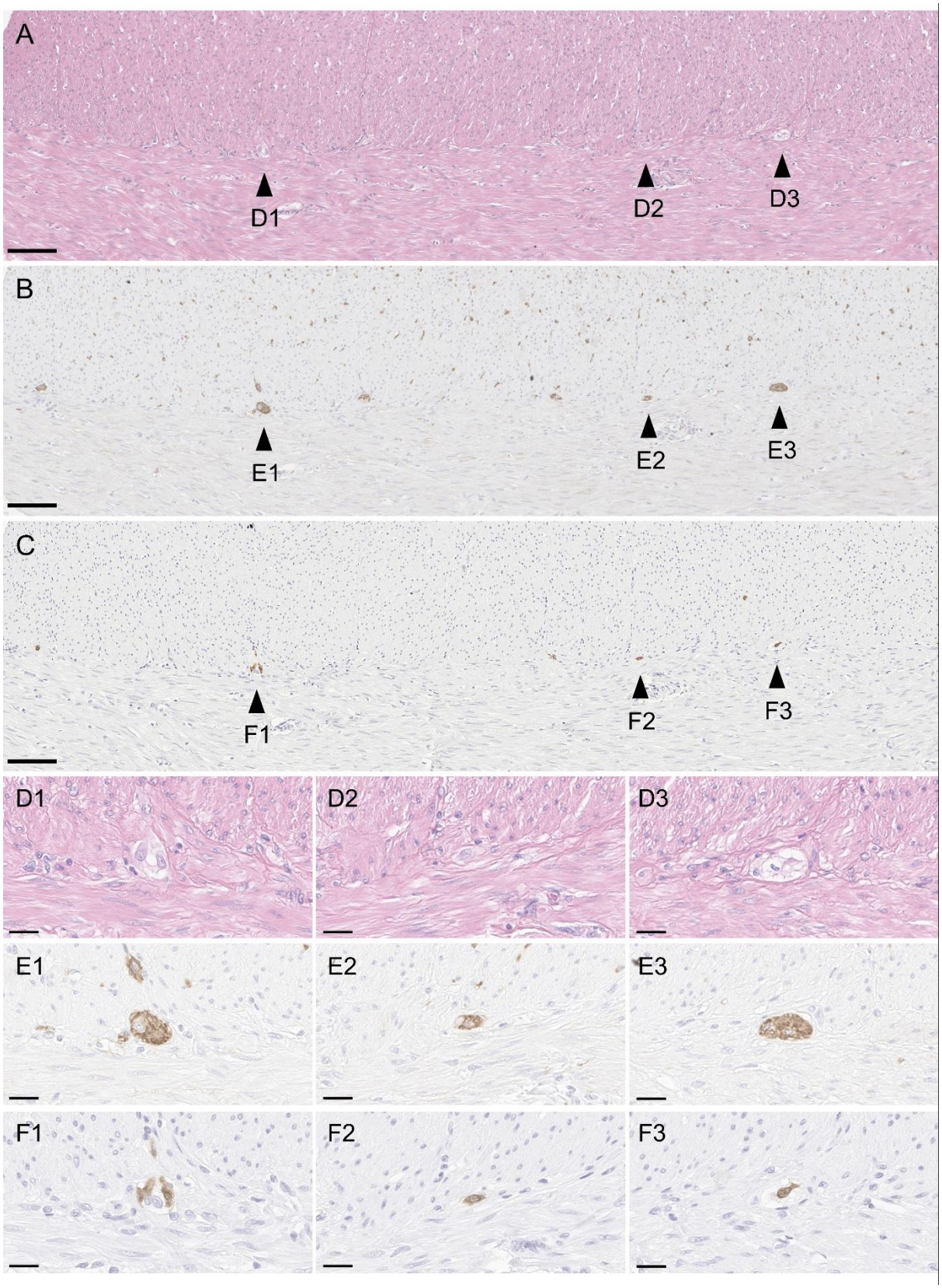

409

410 **FIUGURE 2A.**

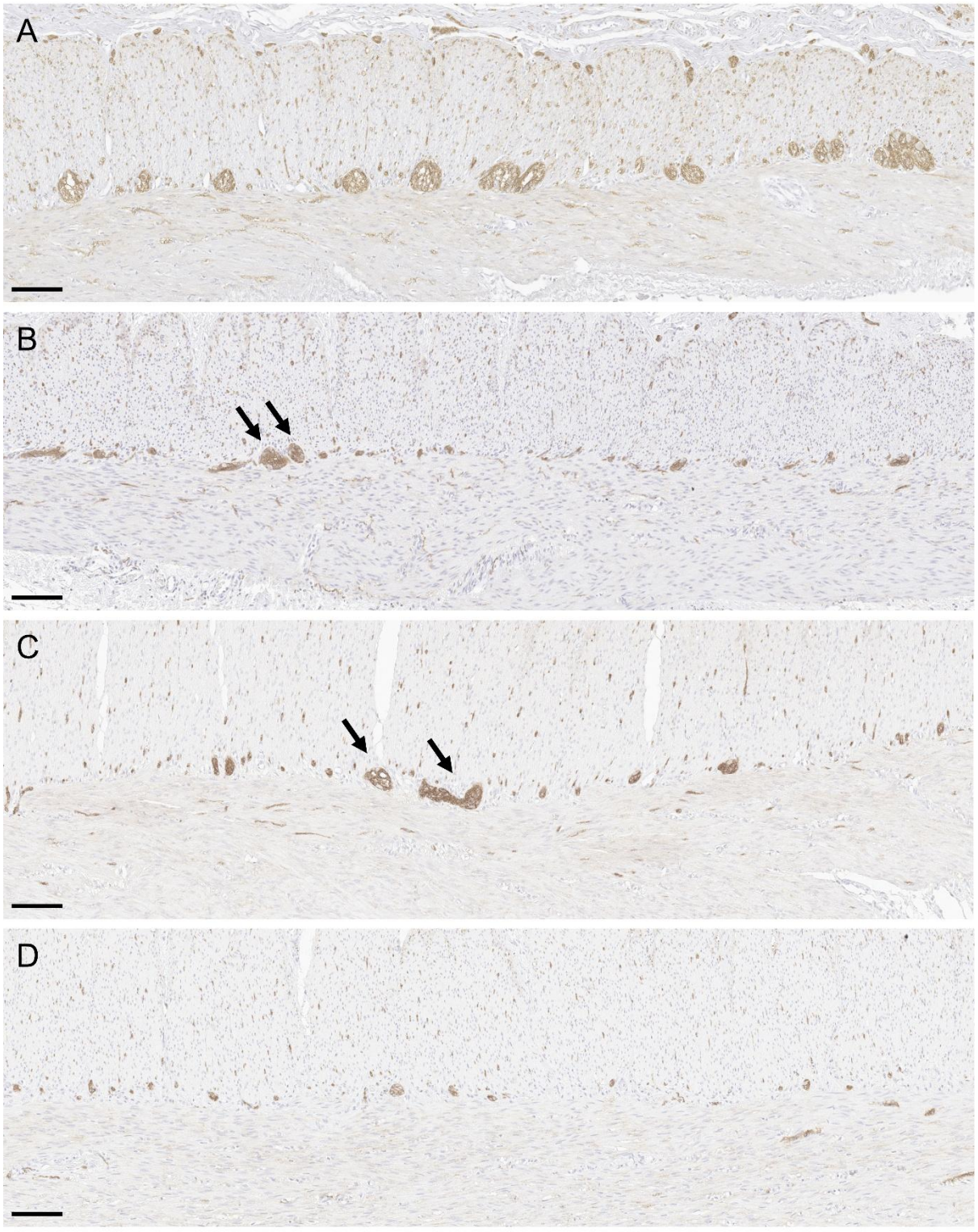

411

FIGURE 2B.

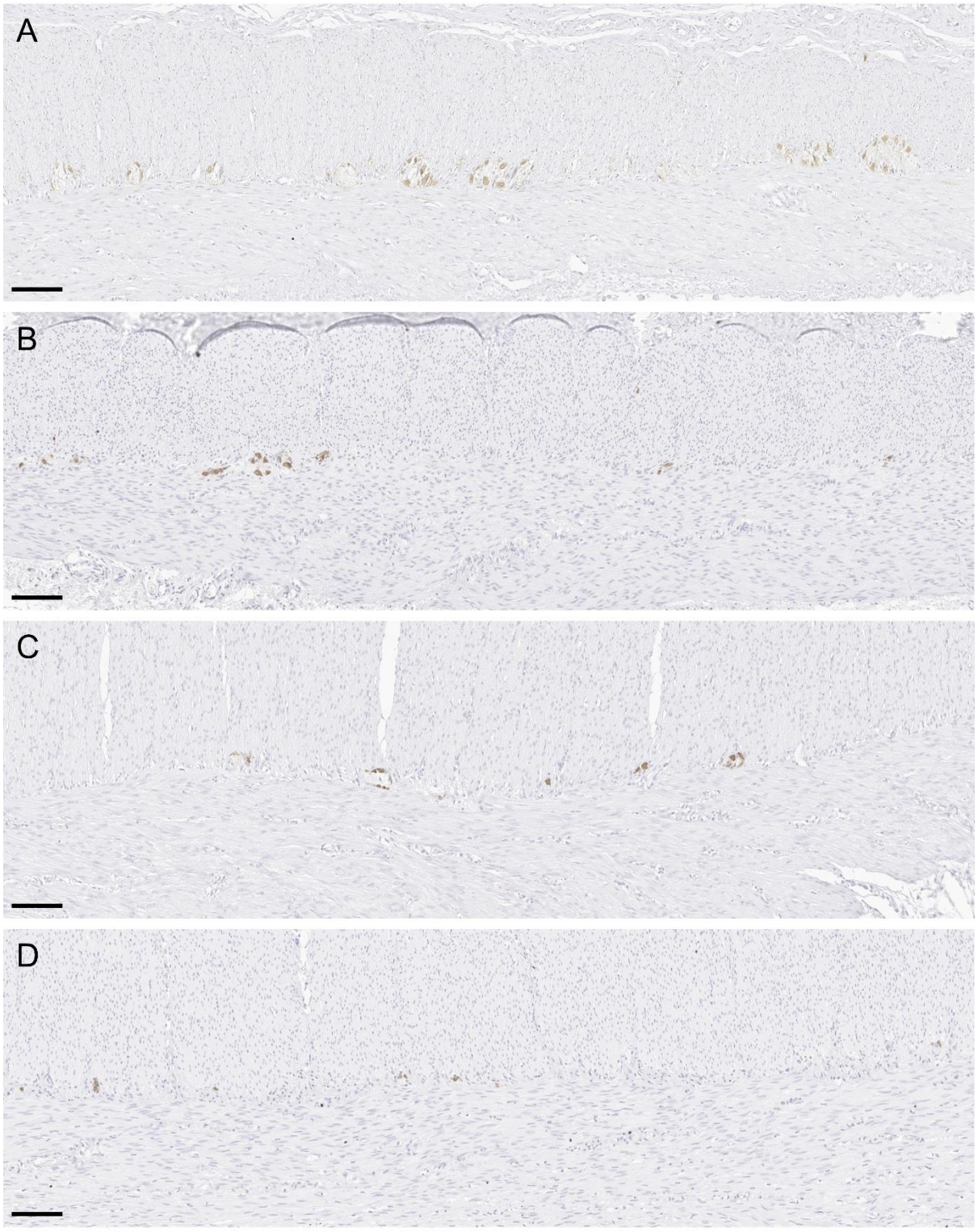

414 **FIGURE 3.**

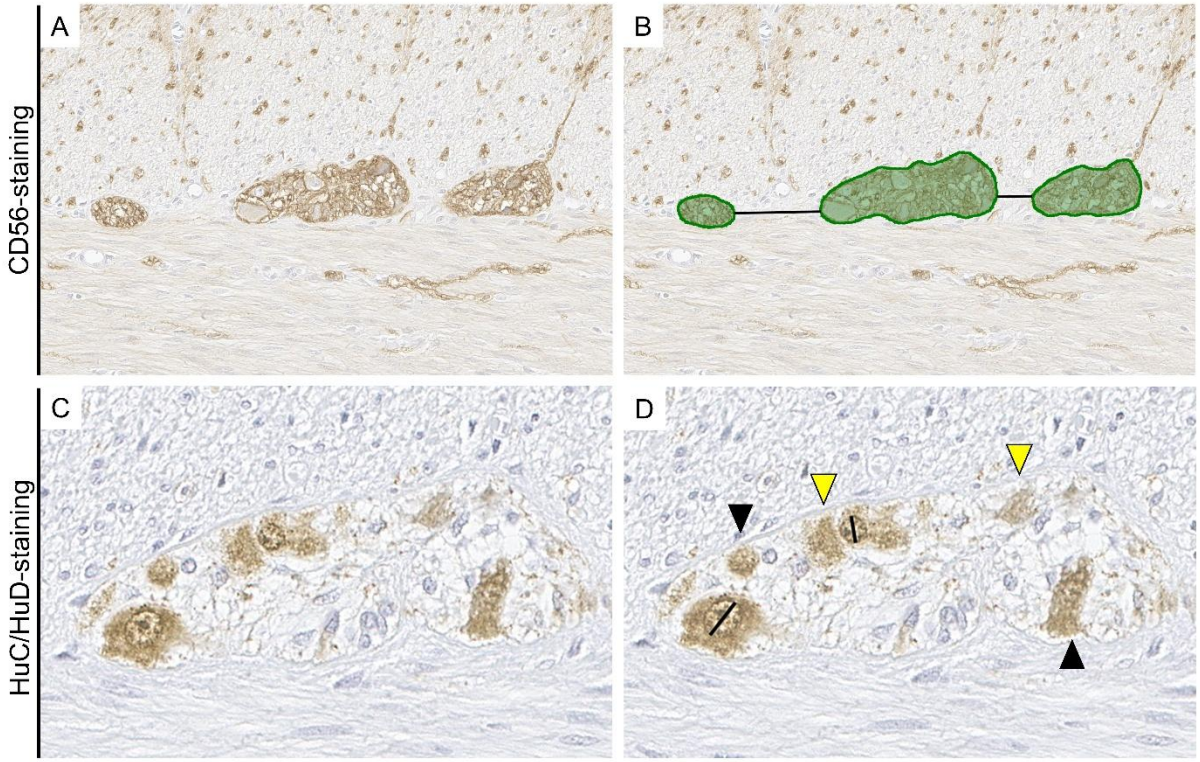

415
416

417 **FIGURE 4.**

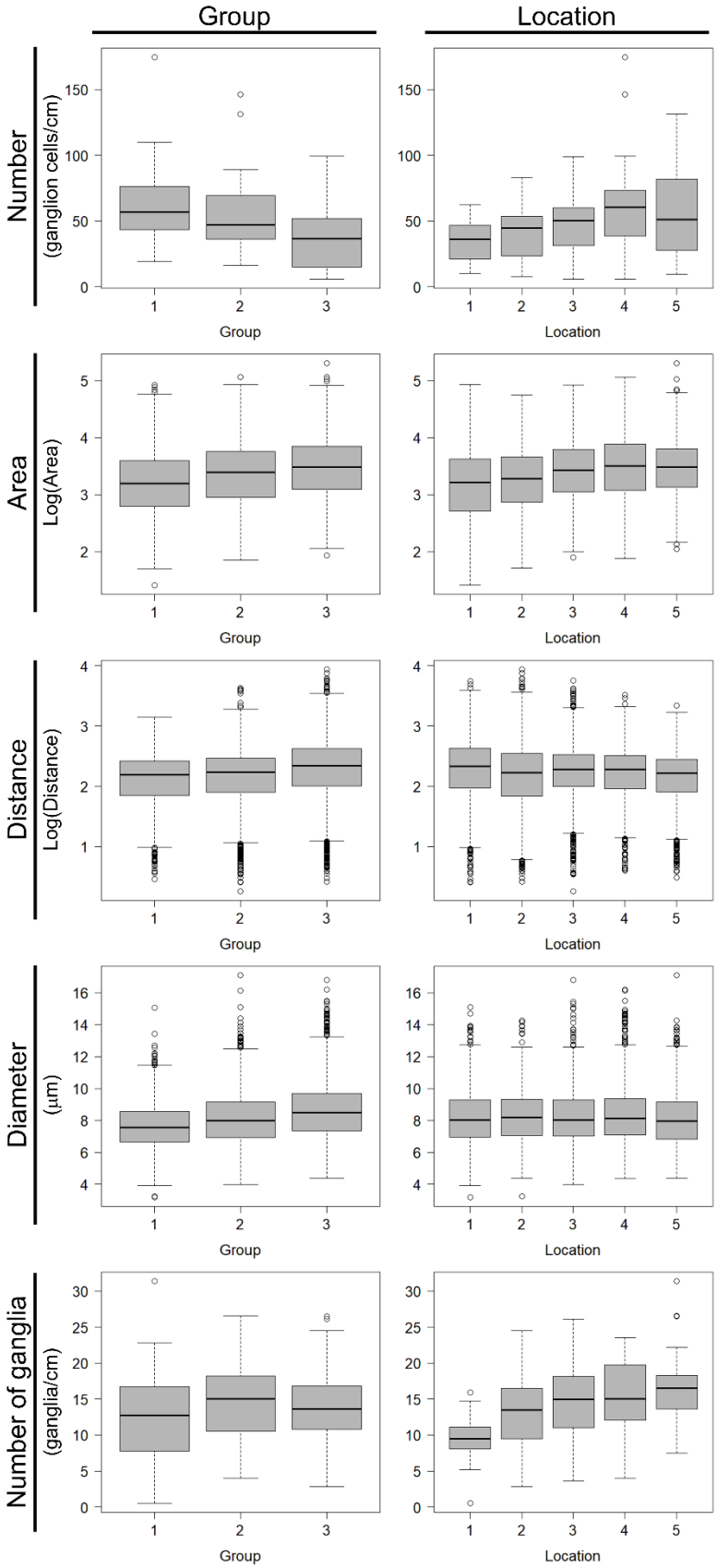

418
419
420

421 **FIGURE 5.**

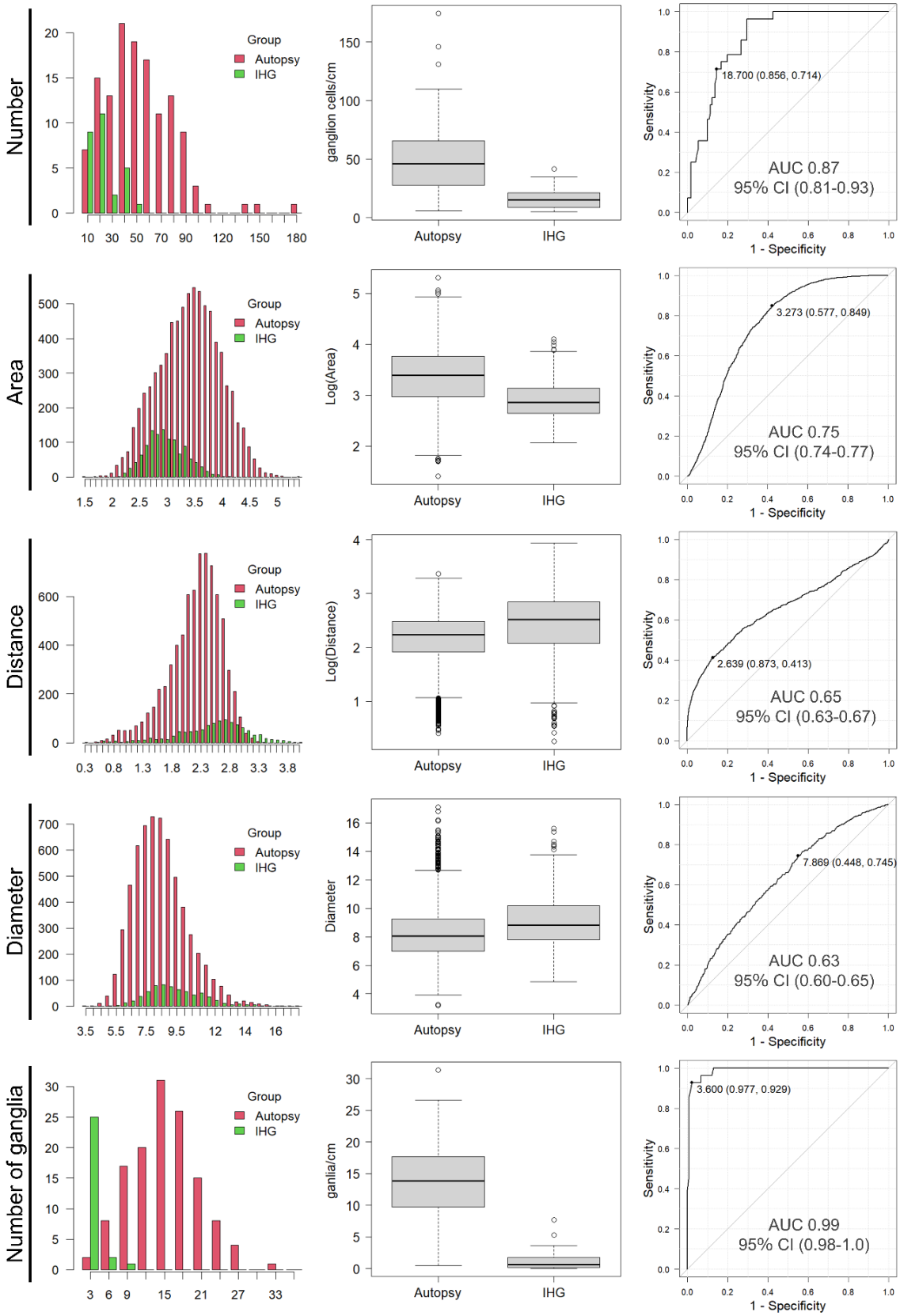

422
423

FIGURE LEGENDS

FIGURE 1. Histological Findings of the Myenteric Plexus in a Case of IHG (case 4; age, 23 months).

The image shows a transverse colon section in an IHG case. The myenteric ganglia (black arrowheads, D1-F3) are small and sparse. Higher-magnification images of each ganglion are shown below (D1-F3). Each image shows hematoxylin and eosin (H&E) stained sections (A, D1-D3) and immunostained sections of the same part of the H&E-stained sections (B and E1-E3, CD56-stained sections; C and F1-F3, HuC/HuD-stained sections).

IHG, isolated hypoganglionosis; H&E, hematoxylin and eosin.

Scale bars: A-C, 100 μm; D1-F3, 20 μm.

FIGURE 2A. Comparison of Myenteric Ganglia Distribution between an Autopsy Case (A, case 5; age, 6 months) and IHG Cases (B, case 1; age, 30 months; C, case 2; age, 3 months; D, case 4; age, 23 months).

In IHG cases, most of the myenteric ganglia are smaller than those in the autopsy case, but some IHG cases have relatively larger myenteric ganglia (black arrows). A–D: CD56-immunostained sections.

Scale bars: A–D, 100 μm.

FIGURE 2B. Comparison of Myenteric Ganglion Cell Distribution between an Autopsy Case (A, case 5; age, 6 months) and IHG Cases (B, case 1; age, 30 months; C, case 2; age, 3 months; D, case 4; age, 23 months).

IHG cases have fewer and sparser myenteric ganglion cells than the autopsy case does. A–D: HuC/HuD-immunostained sections.

Scale bars: A–D, 100 μm.

FIGURE 3. Immunohistochemical Findings of the Myenteric Ganglia and Ganglion Cells to be Measured (A, C), and Schematic Diagrams of the Measurements (B, D).

Myenteric plexus components in the ileum from autopsy case 5 (patient age, 6 months). B, Green areas show the measured area of the myenteric ganglia, and black lines show the measured distance between ganglia. D, Black lines indicate the diameter of the nucleus of the myenteric ganglion cells. Black arrowheads show ganglion cells that were only counted in number and not measured in diameter because the nuclear outline of these ganglion cells was partially obscured. Yellow arrowheads show the brown-stained area that was not counted due to the blurred nuclear circumference.

FIGURE 4. Summary of Each Parameter in Autopsy Cases in Relation to Age Group and Sampling Site.

None of the parameters showed strong correlations ($r \geq 0.5$) with the age groups or sampling sites. For parameters of the area of the myenteric ganglia and the distance between the myenteric ganglia, box plots were constructed using log-transformed data.

Group 1 includes cases less than 1 month of age; Group 2, 1 month to 1 year; Group 3, over 1 year of age; Number, the number of the myenteric ganglion cells; Area, the area of the myenteric ganglia; Distance, the distance between the myenteric ganglia; Diameter, the diameter of the nucleus of myenteric ganglion cells; Number of ganglia, the number of myenteric ganglia with an area >2500 μm^2. Location 1, jejunum; Location 2, ileum; Location 3, ascending colon; Location 4, transverse colon; Location 5, rectum.

FIGURE 5. Comparison of Autopsy and IHG Cases.

The parameters that showed high diagnostic accuracy (AUC ≥ 0.7, sensitivity ≥ 0.7, specificity ≥ 0.7) were the number of ganglion cells/cm and number of myenteric ganglia with area >2500 μm^2/cm. Using log-transformed data, we created histograms and box plots and performed ROC analyses for the area of myenteric ganglia and the distance between myenteric ganglia.

IHG, isolated hypoganglionosis; number, number of myenteric ganglion cells; area, area of the myenteric ganglia; distance, distance between the myenteric ganglia; diameter, diameter of the myenteric ganglion cell nucleus; ROC, receiver operator characteristic; AUC, area under the curve; CI, confidence interval.

484 **TABLES**
485

TABLE 1. Scoring system

Number of myenteric ganglion cells (/cm)	<10	10≤, <20	20≤, <50	50≤
N-Score	2	1	0	-1
Number of myenteric ganglia (≥2500μm^2) (/cm)	0≤, <3	3≤, <6	6≤, <10	10≤
S-Score	2	1	0	-1

486
487

TABLE 2. Clinical Characteristics of Autopsy Cases and IHG Cases

Variable	Autopsy	IHG
Total (n)	29	10
Sex (Males/Females)	17/12	5/5
Age (mo), median (range)	6 (0–119)	32 (3–230)
Age group, n (%)		
Group 1 (< 1 mo)	6 (21)	0 (0)
Group 2 (1 mo ≤, <12 mo)	11 (38)	2 (20)
Group 3 (12 mo ≤)	12 (41)	8 (80)
Location of sampling sites, n (G1/G2/G3)		
Jejunum	25 (5/9/11)	4 (0/2/2)
Ileum	25 (5/8/12)	10 (0/2/8)
Ascending colon	28 (6/10/12)	7 (0/1/6)
Transverse colon	27 (6/9/12)	5 (0/0/5)
Rectum	27 (6/9/12)	2 (0/0/2)
Cause of Death, n (%)		
Neoplasms	2 (7)	-
Heart disease	6 (21)	-
Respiratory disease	1 (3)	-
Congenital anomalies	4 (14)	-
Infections	3 (10)	-
Others	13 (45)	-

Age is expressed as months at the time of autopsy or operation.
IHG, isolated hypoganglionosis; G1, Group 1; G2, Group 2; G3, Group 3.

TABLE 3. Comparison of Medians for Each Parameter Between Autopsy and IHG Cases

Variables	Autopsy	IHG	*P*-value
Number, median (ganglion cells/cm) (IQR)	45.9 (28.5–65.7)	15.1 (9.0–20.8)	< 0.001*
Area, median (μm^2) (IQR)	2448.5 (942.7–5797.5)	718.2 (440.5–1372.5)	< 0.001*
Distance, median (μm) (IQR)	173.4 (82.1–303.6)	326.4 (118.7–704.1)	< 0.001*
Diameter, median (μm) (IQR)	8.0 (6.9–9.2)	8.8 (7.7–10.1)	< 0.001*
Number of ganglia, median (ganglia/cm) (IQR)	13.9 (9.9–17.7)	0.7 (0.3–1.7)	< 0.001*

IHG, isolated hypoganglionosis; Number, the number of the myenteric ganglion cells; Area, the area of the myenteric ganglia; Distance, the distance between the myenteric ganglia; Diameter, the diameter of the nucleus of myenteric ganglion cells; Number of ganglia, the number of myenteric ganglia with an area greater than 2500 μm^2; IQR, interquartile range.
*$P < 0.05$.

TABLE 4. Scores of IHG cases by the scoring system

Case (age, mo)	The number of ganglion cells (/cm)	N-score	The number of ganglia (/cm)	S-score	Total score
Case 1 (30)					
Jejunum	13.4	1	0	2	3*
Ileum	20.3	0	0.3	2	2*
A-colon	10.3	1	0.7	2	3*
T-colon	12.6	1	5.3	1	2*
Rectum	34.7	0	1.9	2	2*
Case 2 (3)					
Jejunum	34.7	0	7.7	0	0
Ileum	18.0	1	2.8	2	3*
Case 3 (8)					
Jejunum	7.7	2	0.3	2	4*
Ileum	6.9	2	0	2	4*
A-colon	18.7	1	0	2	3*
Case 4 (23)					
Ileum	15.0	1	0	2	3*
A-colon	22.3	0	0.3	2	2*
T-colon	31.3	0	2.5	2	2*
Case 5 (60)					
Ileum	18.0	1	3.6	1	2*
A-colon	7.7	2	0.9	2	4*
T-colon	16.0	1	0.3	2	3*
Case 6 (27)					
Ileum	34.5	0	1.5	2	2*
A-colon	12.7	1	0.6	2	3*
Case 7 (33)					
Ileum	7.2	2	0.1	2	4*
Case 8 (48)					
Ileum	4.8	2	0	2	4*
Case 9 (46)					
Ileum	15.2	1	0	2	3*
A-colon	30.9	0	1.3	2	2*
T-colon	41.6	0	1.6	2	2*
Case 10 (230)					
Jejunum	5.5	2	0.5	2	4*
Ileum	6.5	2	2.0	2	4*
A-colon	10.0	1	0.9	2	3*
T-colon	9.5	2	1.6	2	4*
Rectum	18.4	1	0.5	2	3*

*Total score $\geq$2. IHG, isolated hypoganglionosis.
The number of ganglion cells, the number of myenteric ganglion cells; The number of ganglia, the number of myenteric ganglia with an area greater than 2500 μm^2.

492